Dynamical scaling of surface growth in simple lattice models

S. Pal,[1,*] D. P. Landau,[2] and K. Binder[3]
[1]*Department of Physics, Pennsylvania State University, University Park, Pennsylvania 16802, USA*
[2]*Center for Simulational Physics, The University of Georgia, Athens, Georgia 30602, USA*
[3]*Institut für Physik, Universität Mainz, Staudinger Weg 7, D-55099 Mainz, Germany*
(Received 22 August 2002; published 7 August 2003)

We present extensive simulations of the atomistic Edwards-Wilkinson (EW) and Restricted Edwards-Wilkinson (REW) models in $2+1$ dimensions. Dynamic finite-size scaling analyses of the interfacial width and structure factor provide the estimates for the dynamic exponent $z=1.65\pm0.05$ for the EW model and $z=2.0\pm0.1$ for the REW model. The stochastic contribution to the interface velocity U due to the deposition and diffusion of particles is characterized for both the models using a blocking procedure. For the EW model the time-displaced temporal correlations in U show nonexponential decay, while the temporal correlations decay exponentially for the REW model. Dynamical scaling of the temporal correlation function for the EW model yields a value of z, which is consistent with the estimate obtained from finite-size scaling of the interfacial width and structure factor.

DOI: 10.1103/PhysRevE.68.021601 PACS number(s): 81.15.Aa, 81.10.−h, 05.40.−a, 05.10.−a

I. INTRODUCTION

The diverse morphologies of thin films growing on solid surfaces by vapor deposition are controlled by nonequilibrium kinetics instead of equilibrium thermodynamics. Competition between deposition and diffusion of atoms on surfaces produces nonequilibrium surface fluctuations, which, in turn, determine the film structure. At long times and large length scales, the structures produced by the deposition of atoms on *different* substrates often appear similar [1], and therefore it is believed that a unique dynamics can characterize the growth behavior in these dissimilar systems. During the past decade significant effort has been expended on the improvement of understanding of these ''generic'' morphological features of surface growth, as well as the characteristic nonequilibrium surface fluctuations that produce these, using simple atomistic growth models and continuum growth equations [2]. Due to the complex nature of the growth process, obtaining an understanding of the dynamics that produce these generic surface fluctuations has been challenging. Although continuum growth equations have provided insight into the possible nature of the fluctuations, much still remains to be understood, *including the effect of long-range temporal correlations on growth behavior*. In this paper we explore this special aspect of surface growth through computer simulations of two quite simple atomistic (lattice) growth models: the $(2+1)$-dim Edwards-Wilkinson (EW) model, which is a simple lattice realization of the physical description underlying the Edwards-Wilkinson equation, and the ''restricted'' Edwards-Wilkinson (REW) model [3], which differs from the EW model by a simple, but important, modification of the diffusion rule. The EW model has been studied previously by computer simulation [4]; but we shall show that, presumably due to the limited computer resources available at that time, this earlier study arrived at the wrong conclusions.

Remarkably, long-range temporal correlations are observed in a diverse array of driven systems far from equilibrium, from semiconductor resistors [5,6] and superconductor Josephson junctions [7] to the information superhighway [8]. Numerical simulations of a nonlinear growth equation developed by Kardar, Parisi, and Zhang (KPZ) [9] have shown that long-range temporal correlations in the velocity of the fluctuating interface are present [10]. These manifest themselves as power-law divergences in the low-frequency fluctuation spectrum. Also, another form of temporal correlations in surface growth has been investigated using the KPZ equation [9] and has been discussed in Ref. [11]. Medina *et al.* [11] derived growth exponents as a function of a parameter that characterized the decay of temporally correlated noise.

In a growing surface, two correlation lengths $\xi_\parallel$ and $\xi_\perp$ develop as the surface structure evolves in time. The parallel correlation length $\xi_\parallel$ is typically the size of long-wavelength structures on the surface and increases with time. In addition, the perpendicular correlation length $\xi_\perp$ which is proportional to the interfacial width, grows with time. When $\xi_\parallel$, and $\xi_\perp$ have grown to scales that are larger than atomistic lengths, but much smaller than the size of the system, some universal growth laws and dynamical scaling behavior, characteristic for a few universality classes, are expected [2,12]. One purpose of this study is to probe such concepts. If growth is continued for long enough time, then $\xi_\parallel \sim L$, where L is the lateral extent of the system, and $\xi_\perp$ also reaches a saturated value. Because spatial correlations reach static values, interface shape fluctuations should become time invariant and any long-range temporal correlations, if present, will vanish. These observations serve as the basic premise of this study.

In the following section we will describe the atomistic EW and REW growth models and also provide a general scaling theory of the interfacial width and the structure factor. In addition, we will introduce a dynamical quantity $U(t)$, which will be used to characterize the (possibly transient) stochastic contribution to the interface velocity during

*Present address: SciMax Research, P.O. Box 0015, Mountain View, California 94042-0015, USA.

growth. Measurement of the surface properties such as the interfacial width, structure factor, and U are discussed in Sec. III. The results for the interfacial width and structure factor for the EW and REW models are presented in Sec. IV, as are data for the surface stiffness λ and stochastic contribution to the interface velocity U, and all properties are then analyzed using dynamic finite size scaling. Section V includes discussion and the conclusion appears in Sec. VI.

II. THEORETICAL BACKGROUND AND MODELS

A. Atomistic EW and REW models

The EW model describes the growth of a random interface above a substrate onto which particles are randomly deposited by a stochastic flux. The mathematical description of this process is given in terms of a linear Langevin equation [13–15]

$$\frac{\partial h}{\partial t} = \nu \nabla^2 h + \zeta, \tag{1}$$

where $h(\mathbf{r},t)$ is the deviation of the height of the interface above the substrate at time t and at position $\mathbf{r}$ from its average value. The coefficient ν is the surface tension, and ζ is the noise term of the random deposition process. In the original EW formulation [15] the noise is taken to be δ correlated in space and time, but due to the linearity of Eq. (1), the treatment could easily be generalized to take into account correlations of the noise. It is these possible correlations that are of interest in the context of our study, as we shall try to identify the individual terms of Eq. (1) directly from the simulations. Indeed, we shall find that the term in ζ is strongly correlated. Taking the spatial and temporal fourier transform $h(\mathbf{k},\omega)$ of $h(\mathbf{r},\mathbf{t})$ we find that the height-height correlations can be formally expressed in terms of the noise correlations as follows:

$$\langle h(\mathbf{k},\omega) h(\mathbf{k}',\omega') \rangle = \frac{\langle \zeta(\mathbf{k},\omega) \zeta(\mathbf{k}',\omega') \rangle}{(\nu k^2 - i\omega)(\nu k'^2 - i\omega')}. \tag{2}$$

For the EW equation, it is easy to derive the growth exponent $z=2$ (see also Secs. II B and II C below), but it turns out that this description is too simplified and does not capture the actual behavior of many atomistic growth models. On a continuum level, an important feature that is not contained in Eq. (1) is nonlinearity. For example, the growth equation suggested by KPZ [9] ammends Eq. (1) by adding a term proportional to $(\nabla h)^2$. Such a correction term describes the fact that the macroscopic growth rate depends on the surface tilt [12]. Such nonlinearities lead to long-range height-height correlations both in space and time beyond those that can be described by Eqs. (1) and (2), and they lead to a nontrivial value of the dynamic exponent z (which then also depends upon the dimensionality of the system).

Various atomistic deposition models (e.g., Refs. [16–25]) have been studied, and some of them (such as Ref. [4]) have been interpreted as being an atomistic version of the EW model. As we shall demonstrate in this paper, it is a subtle matter to ascertain whether or not a particular atomistic model is equivalent to the linear EW equation, since effective nonlinearities could be generated in the coarse-graining procedure. In addition, as we shall show below, some of the claims made for the values of the dynamic exponent [4] are invalid, presumably because the early work was restricted to too small a range of lattice sizes.

In the present paper we focus on two atomistic models, which we call the ''atomistic EW model'' and the ''restricted EW (REW) model.'' To simulate the atomistic EW model we begin with a flat $L \times L$ substrate with periodic boundary conditions. Particles are randomly deposited on the surface and time t in the simulation is measured in units of the number of monolayers deposited. Only a freshly deposited particle can move just after it is deposited, but only *once*, to a nearest-neighbor column with a minimum height if such a site is available. In case two or more available sites have the same minimum height, the final site is chosen randomly.

In the REW model [3] a freshly deposited particle moves to a nearest-neighbor column with the minimum height if such a site is uniquely defined. If several such sites are available, the deposited particle does not move to any of them, but stays instead where it was initially deposited! At this point it appears as though the distinction between our REW model and the original ''atomistic EW model'' is an irrelevant detail; but as we shall show later, only the REW model can serve as an atomistic version of the EW equation. The ''atomistic EW model'' seems to belong, instead, to a different universality class of growth models. Thus, in contrast to the EW model no move is allowed if two or more equally deep sites are present.

B. Scaling theory of interfacial width

To characterize the surface fluctuations in a given growth model, traditionally interfacial widths have been measured. This is a simple and elegant approach to describe the surface dynamics when growth proceeds to long times, but recent studies suggested that for intermediate times lattice step density gave better agreement with a continuum theory of surface fluctuations [26]. The interface fluctuations in the atomistic EW and REW models have been characterized by measuring the interface width $W(L,t)$, where

$$W^2(L,t) = [\langle h^2(\mathbf{r},t) \rangle - \langle h(\mathbf{r},t) \rangle^2], \tag{3}$$

$\langle h(\mathbf{r},t) \rangle = L^{-d} \Sigma_r h(\mathbf{r},t)$, L is the lateral extent of the system, d is the interface dimensionality and $\langle \cdots \rangle$ denotes ensemble average. In general, the width $W(L,t)$ of a kinetically roughened surface evolves according to the dynamic scaling law [13]

$$W^2(L,t) = L^{2\alpha} f\left(\frac{t}{L^z}\right), \tag{4}$$

where the exponent α characterizes the surface fluctuations in a given growth model and z is the dynamic exponent. The scaling function has the property $f(x) \sim x^{\alpha/z}$, for $x \ll 1$ and

$f(x) \rightarrow$ const, for $x \gg 1$. Solution of Eq. (1) gives $\alpha = 0$ for two-dimensional interfaces, and $z=2$ independent of the interface dimensionality.

The linear Langevin equation [Eq. (1)]) has been solved exactly by Nattermann and Tang [27] who derived expressions for the interfacial width and structure factor. We have used these theoretical solutions to define the dynamical scaling relations in the atomistic models. For long time t and large substrate sizes L, the interfacial width $W(L,t)$ is expected to satisfy the dynamic scaling relation [28]

$$W^2(L,t) = A \ln\left[L f\left(\frac{t}{L^z} \right) \right], \tag{5}$$

where $f(x)$ is the scaling function, z is the dynamic exponent, and A is a constant. The scaling function has the property $f(x) \sim x^{\beta}$, for $x \ll 1$ and $f(x) \rightarrow$ const, for $x \gg 1$. The exponents z and β satisfy the relation

$$z\beta = 1. \tag{6}$$

Thus for small t and large L, the interfacial width behaves as $W^2 \sim A\beta \ln t$, while for very long times it saturates at a value (W_{∞}) and $W_{\infty}^2 - A \ln L \sim$ const.

C. Scaling theory of structure factor

The surface dynamics can also be characterized by measuring the structure factor, which provides information about the surface at different length scales. The structure factor $S(qL,L,t)$ can be obtained from the Fourier transform of the spatial correlation function,

$$S(qL,L,t) = L^{-d} \sum_{\mathbf{r},\mathbf{r}'} H(\mathbf{r},t) H(\mathbf{r}',t) \exp[i\mathbf{q}\cdot(\mathbf{r}-\mathbf{r}')], \tag{7}$$

where $H(\mathbf{r},t) = h(\mathbf{r},t) - \langle h(\mathbf{r},t) \rangle$, $qL = 2n\pi$, and n is an integer. The structure factor should satisfy the dynamic scaling law [29],

$$S(qL,L,t) = L^{(2-\eta)} g(t/L^z, qL), \tag{8}$$

where η is an exponent and z is the dynamic exponent. The long-wavelength behavior of the surface can be probed by using a small value of q. In this limit and for large lattice sizes, $g(x,qL) \sim x^{\gamma}$, for $x \ll 1$, and $g(x,qL) \rightarrow$ const, for $x \gg 1$. Here $z\gamma = 2 - \eta$. From the solution of the EW equation, we obtain [27]

$$n^2 S(qL,L,t) = L^2 (D/\nu)[1 - \exp(-8n^2\pi^2 \nu L^{-2} t)], \tag{9}$$

where D and ν are constants. This gives $S(qL,L,t) \sim t$ for $L \rightarrow \infty$ and small t, while at long times $S(qL,L,t \rightarrow \infty) \rightarrow L^2$. This implies that for the EW equation $\eta = 0$, and the exponent identity

$$z\gamma = 2 \tag{10}$$

needs to be satisfied for self-consistency.

D. The stochastic contribution to the interface velocity U

To understand the long-time and large length-scale properties of a dynamical system, a standard approach in critical phenomena is to define a semiphenomenological equation of motion. A small set of semimacroscopic variables ϕ_i, $i = 1,2,\ldots,N$ is used whose dynamical evolution is slow compared to the remaining microscopic degrees of freedom. In these equations [29] the remaining ''fast'' variables enter only in the form of random forces (usually called the noise ζ_i). The equation can be written as

$$\frac{\partial \phi_i}{\partial t} = -\sum M_{ij} \frac{\delta \mathcal{F}}{\delta \phi_j} + \zeta_i, \tag{11}$$

where $\mathcal{F}$ is the Ginzburg-Landau coarse-grained free energy functional and M is the matrix of generalized Onsager coefficients. Depending on the models studied [29], the noise can have spatial correlations, and for equilibrium systems the noise is δ correlated in time. The EW equation is a simple extension of the above approach where the noise is δ correlated in time, and the semimacroscopic variable is the height $h(\mathbf{r},t)$ of the surface.

Since in the presence of an external field, such as a random flux, the system is driven away from equilibrium, it may be necessary to include additional terms in Eq. (1) to correctly account for any effects due to deposition. The interplay of the flux and surface diffusion can cause complex behavior at long times and large length scales, and so these terms are often difficult to construct accurately. For simplicity we assume that any additional terms to the growth equation, if present, can be included in a new, general function U, which we term the stochastic contribution to the interface velocity. Apart from any relevant surface shape gradients, such a term includes the random contribution due to the flux, and spatiotemporal couplings that may be important to the growth behavior at long times and large length scales. Thus, the simplest form of the growth equation may be written as

$$\frac{\partial h(\mathbf{r},t)}{\partial t} = \lambda \nabla^2 h(\mathbf{r},t) + U(\mathbf{r},t), \tag{12}$$

where λ is a measure of the surface stiffness, which changes with time as the surface grows. The physical meaning of the stochastic contribution to the interface velocity U may be understood by comparing Eq. (12) with Eq. (1). In Eq. (1) the interface velocity $\partial h/\partial t$ does not fully include the effects that diffusion may cause to the interface degrees of freedom. Thus, the translation of the interface due to growth does not accurately produce appropriate surface fluctuations. These effects are fully included in Eq. (12).

In general, U should capture representative information about system dynamics in an atomistic growth model if one of the surface gradients contributing to the asymptotic behavior is the curvature. The dynamics of the atomistic model and the continuum equation (12) may then be compared to obtain a measure of U. If the behaviors of the atomistic model and the EW equation (1) are the same, the stochastic contribution to the interface velocity (U) should be random in both space and time. An elegant way to determine, if this

is the case, is to calculate its space and time-displaced correlation functions. This, in turn, will elucidate if any nontrivial correlations relevant to the long-time and large length-scale dynamics are present in the system.

III. MEASUREMENT OF SURFACE PROPERTIES

The surface fluctuations in the EW and REW models are characterized by measuring the interfacial width [cf. Eq. (3)] and the structure factor [defined by Eq. (7)]. The structure factor is measured along the (1,0) and (0,1) directions and averaged over these directions.

To measure the stochastic contribution to the interface velocity during growth, we write Eq. (12) in a discrete form. The time derivative of $h(\mathbf{r},t)$ becomes

$$\frac{\partial h(\mathbf{r},t)}{\partial t} = \frac{h(\mathbf{r},t+\Delta t) - h(\mathbf{r},t-\Delta t)}{2\Delta t}, \tag{13}$$

where t is normally equal to the number of monolayers deposited unless another unit has been specified. Note that each monolayer corresponds to the deposition of $L \times L$ particles. The curvature of the surface at position $\mathbf{r}$ can be written as a finite difference formula

$$\nabla^2 h = h(x,y+1) + h(x+1,y) + h(x-1,y) + h(x,y-1) - 4h(x,y), \tag{14}$$

where $\mathbf{r} = \boldsymbol{i}x + \boldsymbol{j}y$, $\boldsymbol{i},\boldsymbol{j}$ are unit vectors on the two-dimensional surface. During growth, we calculate two quantities: $Q_1 = \langle \partial h/\partial t \rangle_{\mathbf{r}}$ and $Q_2 = \langle \nabla^2 h \rangle_{\mathbf{r}}$, where $\langle \cdots \rangle_{\mathbf{r}}$ denotes an average over space within a given block size b, at a given time t. An estimate of the stiffness of the surface $\lambda(b,t)$ is then obtained by taking the ratio Q_1/Q_2. To obtain $U(\mathbf{r},t)$ we put the value of the surface stiffness λ back into Eq. (12). Equating the left- and right-hand sides of the equation we can calculate the dynamical contribution to the interface velocity

$$U(\mathbf{r},t) = \frac{\partial h(\mathbf{r},t)}{\partial t} - (Q_1/Q_2)\nabla^2 h, \tag{15}$$

at a given time t for *each* site. Here $\partial h(\mathbf{r},t)/\partial t$ and $\nabla^2 h$ are given by Eqs. (13) and (14), respectively. To reduce the effect of local spatial correlations, U is averaged over blocks of size b to obtain $U(b,t)$, which then allows us to study its properties over different block sizes for a given L. To study the temporal correlations in $U(b,t)$, we calculate the time-displaced correlation function $C(b,\tau)$. The correlation function is written as

$$C(b,\tau) = \frac{\langle U(b,\tau+t_0)U(b,t_0)\rangle - \langle U(b,t_0)\rangle\langle U(b,\tau+t_0)\rangle}{\langle U^2(b,t_0)\rangle - \langle U(b,t_0)\rangle^2}, \tag{16}$$

where the scaling properties must be independent of t_0. In order to compare with the continuum Edwards-Wilkinson equation we must examine the behavior of the atomistic model for length scales that are much greater than a lattice constant and for long time scales so that the discreteness in space and time are no longer evident. If it turns out that the mean value of U is zero under these conditions, then U is just the stochastic noise of the EW equation. If U is nonzero, the atomistic model should not be expected to have the same behavior as the continuum equation.

Lattice sizes ranging from $L=20$ to $L=1800$ were used for these simulations, and data points were averaged over multiple runs starting with different random number seeds. For the majority of the calculations we used the random number generator RAN2 [30] which has a large period of $\sim 2\times 10^{18}$, and passes standard statistical tests within the limitations of a machine's floating-point representation. Some calculations of the interfacial width were performed using RAN0 [30] where a *new* seed was used in every few thousand random numbers to minimize any serial correlations. RAN0 is about twice as fast as RAN2 but has a small period of $\sim 10^9$ and fails the χ^2 test when the number of random numbers exceed 10^7. A total of about 37 000 CPU hours, using IBM RS/6000 and Pentium processors, were expended on these calculations. Since we required large lattice sizes to clearly establish the scaling properties and a large number of runs to generate data with high accuracy, significant computational resources were a necessity.

IV. RESULTS

A. EW model

Figure 1(a) shows the square of the interfacial width $W^2(L,t)$ versus the number of deposited layers in a semi-logarithmic scale. After an initial transient, up to about 10 layers, the data points crossover to a region where $W^2(L,t)$ evolves logarithmically with t before eventually saturating due to finite system size. The number of runs varied from 50 for $L=1280$ to 2000 for $L=40$, and the error bars (1σ) are about the size of the symbols. Data obtained with a higher temporal resolution show small amplitude oscillations in the interfacial width, but these quickly decay with increasing time and substrate sizes. For $L=640$ and averages over 200 independent runs, the oscillations in the surface width became indistinguishable within statistical fluctuations for growth exceeding ~ 60 monolayers.

Examining the long-time data, we find that the region of logarithmic time evolution grows with increasing lattice size. This is because the parallel correlation length takes a longer time to reach the order of L for larger lattice sizes. The asymptotic behavior is shown as a dotted line that is vertically shifted and shows that the trend extends over three decades for the largest lattice size studied. When we plot the data in a log-log scale, we find systematic curvature, suggesting that the time evolution of $W(L,t)$ is not described by a power-law. The time evolution is logarithmic and can be written as $W^2 \sim A\beta \ln(t)$. The slope of the straight line in the semilogarithmic fit is estimated to be $A\beta = 0.040 \pm 0.001$.

The square of the saturated interfacial width $[W^2(L,t \to \infty) = W_\infty^2]$ also has a logarithmic behavior with L, as shown as an inset in Fig. 1(a). The slope of the best linear fit yields $A = 0.0662 \pm 0.0004$. Using Eq. (6) we estimate the dynamic exponent $z = 1.65 \pm 0.05$. The exact scaling expres-

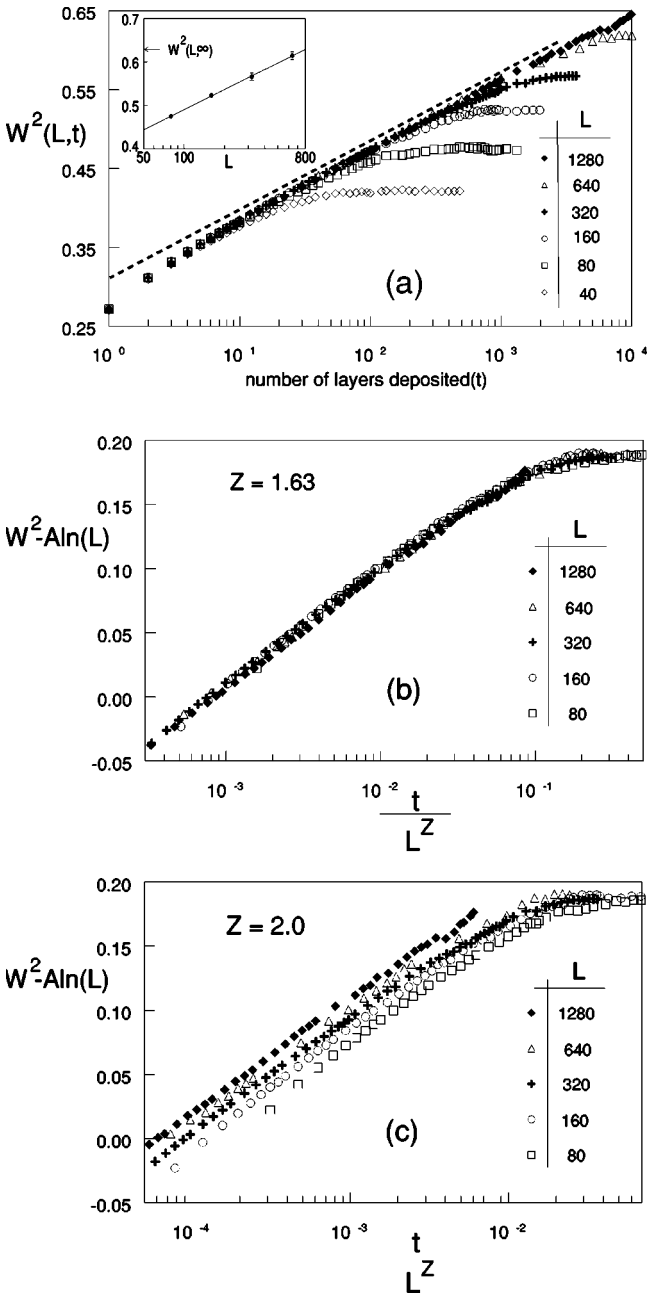

FIG. 1. (a) The square of the interfacial width for the EW model vs the number of deposited layers. The inset shows the variation of the square of the saturated interfacial width (W_∞^2) with lattice size L on a semilogarithmic scale. (b) Dynamical scaling of the interfacial width using $A=0.066$ and $z=1.63$ for the EW model. (c) Dynamical scaling of the interfacial width using $A=0.066$ and $z=2.0$.

sion for the linear EW equation, derived in Ref. [27], can be used to obtain an estimate of the intrinsic width W_0. By referring to Fig. 1(a), we estimate $W_0^2 \sim 0.298$. With just one monolayer of deposition, the interfacial width is already beyond the crossover regime and the estimate of the dynamic exponent z given above is the asymptotic value.

We have verified this estimate for z self-consistently by performing finite-size scaling of the data. Figure 1(b) shows dynamical scaling of the interfacial width with $z=1.63$; excellent collapse of data is achieved with a value for z that is consistent with our previous estimate. With $z=2.0$ scaling failed, as can be seen in Fig. 1(c), systematic deviations appear as larger lattice sizes are used, suggesting that scaling is not obeyed.

When a surface grows it develops structures at different length scales, and at long times only the large-scale surface distortions contribute to the characteristic system dynamics. The structure factor has been measured to characterize these long-wavelength surface distortions. The number of independent runs varied from 4000 to 250 for lattice sizes ranging from $L=40$ to $L=640$, and the error bars are about the size of the symbols. The structure factor data is plotted in Fig. 2(a) on a log-log scale using $qL=2\pi$. The figure shows that $S(qL,L,t)$ has a power law behavior from the first layer deposited and saturates at late times due to finite system size. The asymptotic behavior is shown by the straight dotted line that has a slope $\gamma=1.23\pm0.01$. The inset shows that the saturated structure factor $S(qL,L,t\to\infty)$ behaves as a power of L. A slope of 2.02 ± 0.03 obtained from the log-log plot is consistent with $S(qL,L,t\to\infty)\sim L^2$ according to the scaling relation in Eq. (9). Thus $\eta\sim0$ and, by using Eq. (10), we get $z=1.64\pm0.04$. We have verified this estimate of the exponent to be self-consistent in Fig. 2(b). Collapse of scaled data is achieved with this value of z, validating the dynamic exponent $z=1.65\pm0.05$ obtained from the analysis of the interfacial width. Figure 2(c) shows that an attempt at scaling with $z=2.0$ clearly fails.

At this point, we comment briefly on the conclusion arrived at by Liu and Plischke [4] that $z=2$ for the present model. Their study used much smaller linear dimensions, ranging from $L=30$ to $L=100$; and for such a restricted range of L, we would also not have been able to clearly rule out $z=2$. In order to unambiguously distinguish between different values of the exponent z, a quite large range of L and very good statistical precision are needed.

B. REW model

The square of the interfacial width $W^2(L,t)$ is plotted against time t on a semilogarithmic scale for the REW model in Fig. 3(a). For both the interfacial width and the structure factor, 4000 to 500 independent runs were performed for lattice sizes ranging from $L=40$ to $L=320$. The error bars are about the size of the symbols. The interfacial width $W(L,t)$ shows some curvature up to about 60 layers and then approaches a linear behavior with t. Note that measurements with a higher temporal resolution did not produce any oscillations in the interfacial width as observed for the EW model. At long times the width saturates due to finite system size. The interfacial width behaves as $W^2(L,t)\sim A\beta\ln(t)$ in the linear region, and the slope is given by $A\beta=0.086\pm0.004$. The saturated interfacial width $W^2(L,t\to\infty)$ is also plotted with the substrate sizes L in a semilogarithmic scale, shown as an inset in Fig. 3(a). A straight-line fit through the data points shows that the saturated width varies logarithmically with L, a behavior also observed in the EW model. The slope obtained from the fit is $A=0.173\pm0.002$. Since the REW model has been obtained from the EW model after

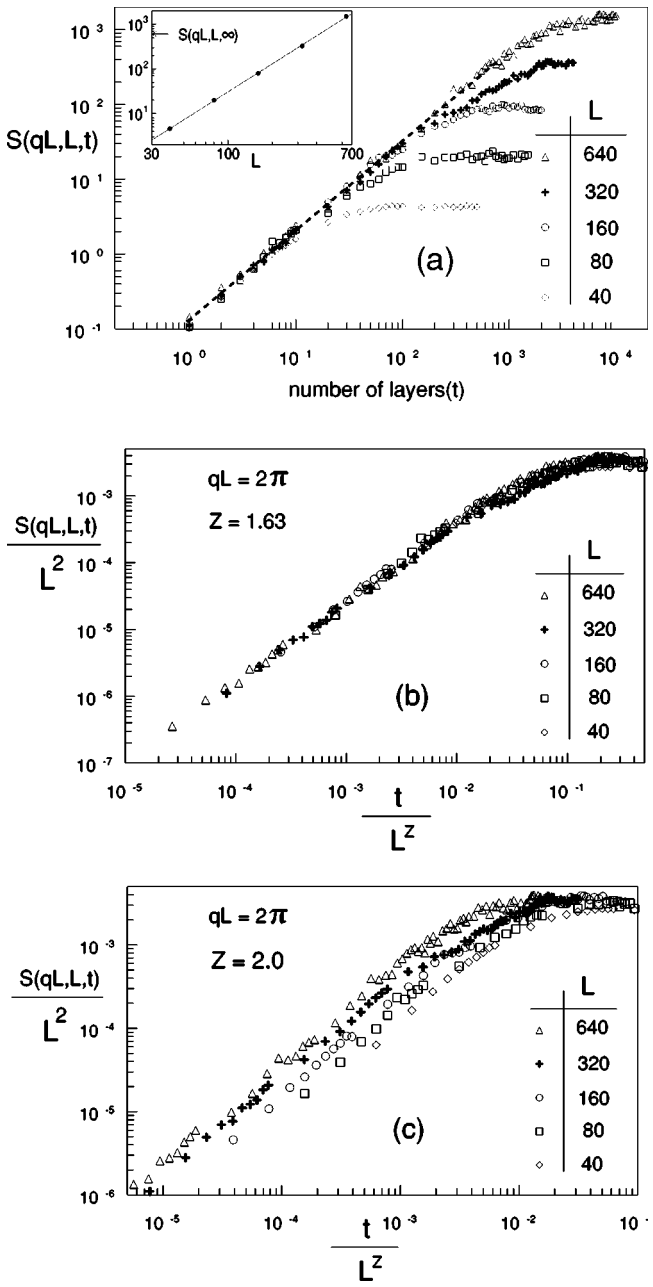

FIG. 2. (a) The structure factor $S(qL,L,t)$ vs the number of deposited layers for the EW model using $qL=2\pi$. The inset shows the saturated values of the structure factor with lattice sizes in a log-log scale. (b) Dynamical scaling of the structure factor in a log-log scale using $z=1.63$. (c) Dynamical scaling of the structure factor for the EW model using $z=2.0$.

minor modifications to the hopping rule, we expect the functional dependence of the interfacial width and the structure factor with time and substrate sizes to be similar. The measurements of the interfacial width have so far demonstrated this agreement. Thus, we assume the scaling theories for the interfacial width and the structure factor developed for the EW model are applicable to the REW model as well. Using Eq. (6) we therefore obtain the exponent $z=2.0\pm0.1$ for the REW model.

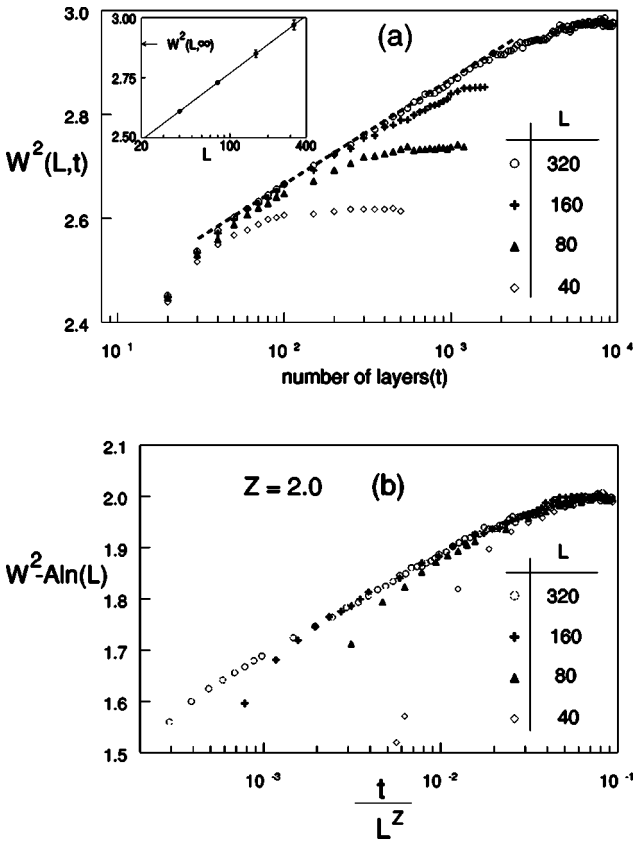

FIG. 3. (a) The square of the interfacial width vs time in a semilogarithmic scale for the REW model. The inset shows the square of the saturated interfacial width $W^2(L,t\to\infty)$ with L in a semilogarithmic scale. (b) Dynamical scaling of the interfacial width using $z=2.0$ and $A=0.173$.

We have tested dynamical scaling for the REW model using $z=2.0$, as shown in Fig. 3(b). The data for small lattice sizes and short times do not collapse. However, a definite trend can be seen in the data with larger lattice sizes, which collapse on to a single curve when growth proceeds to long times. This behavior indicates that dynamical scaling is satisfied by the interfacial width in the limit of long times and large lattice sizes.

The structure factor data are shown in Fig. 4(a) with time t in a log-log scale using $qL=2\pi$. Unlike the behavior of the interfacial width, asymptotic behavior is observed from about the first layer deposited. The asymptotic behavior is indicated by the dashed straight line that has a slope of $\gamma=1.01\pm0.02$, implying a linear evolution of the structure factor. This is similar to the behavior one would expect if growth occurred according to the linear Langevin equation. From the log-log plot of the saturated structure factor with L [inset of Fig. 4(a)], we get $S(qL,L,t\to\infty)\sim L^{(2.03\pm0.04)}$ in agreement with the scaling relation in Eq. (9). Therefore, $\eta\sim0$ and $z=2.01\pm0.08$. In Fig. 4(b) we have tested the dynamical scaling of the structure factor with $z=2.0$. Note that the scaled data for the smaller lattice sizes of $L=40$ and $L=80$ deviate and do not collapse on to a single curve; however, the data for $L=160$ collapse nicely on the $L=320$ data. This suggests that dynamic scaling should be satisfied, as

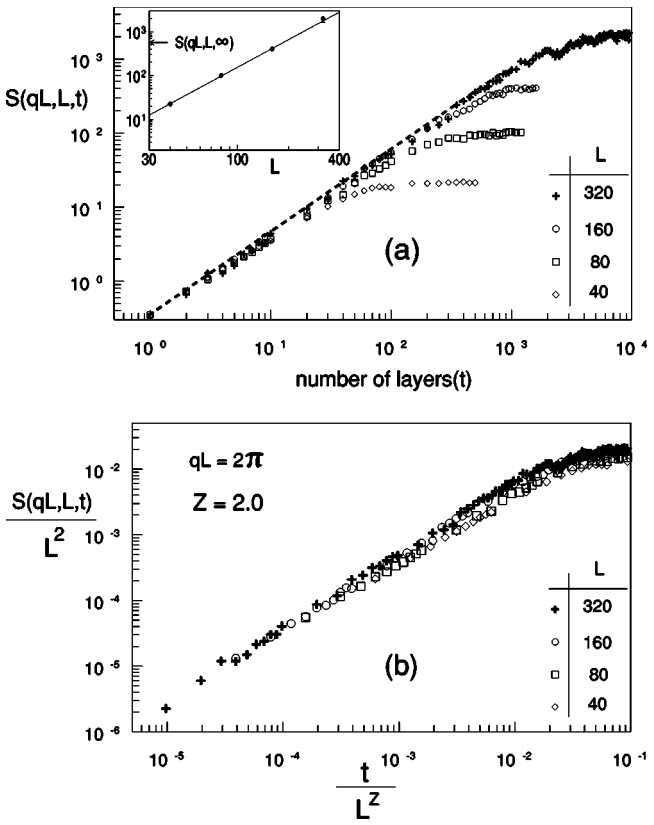

FIG. 4. (a) The structure factor for the REW model using $qL=2\pi$ in a log-log scale. The inset shows the saturated values of the structure factor with L in a log-log scale. (b) Dynamical scaling of the structure factor for the REW model using $z=2.0$.

larger lattice sizes are used with $z=2.0$.

From the measurements of both the interfacial width and the structure factor, we find that the scaling behavior of the REW model is identical to the linear Langevin equation with δ correlated noise [Eq. (1)]. The above results also convincingly demonstrate that the surface fluctuations generated by the deposition of particles in the atomistic EW model are not the same as produced by Eq. (1), and this difference is manifested by different dynamical scaling exponents in these two models.

C. Calculation of U and its properties

In Sec. III we have elucidated the measurement of the stochastic dynamical contribution to the interface velocity $U(b,t)$ and the surface stiffness $\lambda(b,t)$. Figures 5(a) and 5(b) show the time dependence of the surface stiffness $\lambda(b,t)$ and the dynamical contribution to the interface velocity $U(b,t)$ in log-log and linear scales, respectively, for several block sizes. The data for $b=100$, 60, 30, and 15 were averaged over 40, 35, 30, and 30 independent runs, respectively, and the error bars are within the symbol sizes. Both $\lambda(b,t)$ and $U(b,t)$ decay with time t and should saturate due to finite-size effects when large number of layers are deposited. As the surface grows, $\lambda(b,t)$ and $U(b,t)$ initially decay rapidly, with slow decay setting in when large number of layers are deposited. The rate of decay also shows a dependence on the blocksize b. Note that because of very slow decay of $\lambda(b,t)$ and $U(b,t)$ at long times, data with very high accuracy are needed for dynamical scaling studies. Therefore, we will not attempt dynamic scaling of $\lambda(b,t)$ and $U(b,t)$ with our current data.

The slow relaxation can be seen in Fig. 5(c) where we have plotted $U(b,t)$ vs t for $b=100$ up to $t=10\,000$ layers. The data points represent averages over 20 independent runs. After an initial rapid decay, the data appear to saturate when viewed over ~ 3000 layers; however, observations over a much longer time interval reveal a systematic and slow decay in the data. We have modeled the decay in $U(b,t)$, using the general combination of exponential decay and power law

$$f(t)=a_0+a_1 t^{a_2-1}\exp(-a_3 t), \tag{17}$$

where a_0, a_1, a_2, and a_3 are constants. At short times the power law dominates and the behavior is governed by the exponent a_2. For long times the exponential term becomes important.

To compare the response to the interface velocity due to deposition, we have plotted $U(b,t)$ for the EW and REW models with t for $b=30$ in a log-linear scale in Fig. 5(d). The solid circles are data for the atomistic EW model, and the dashed line is $U(b,t)$ for the REW model. The solid line through the data points in solid circles is a fit to Eq. (17). The Levenberg-Marquardt method [30] is used to fit the data points and excellent fit to the data is obtained with high statistical confidence. Equation (17) can therefore be used to model the temporal decay of $U(b,t)$ in the EW model with good accuracy. The fact that U does not decay to zero with time t is surprising: If the stochastic contribution were a random noise, it would vanish on average.

Using Eq. (16) we have computed the normalized time-displaced temporal correlation function $C(b,\tau)$ for the EW and REW models. Figure 6(a) shows $C(b,\tau)$ vs τ in a log-log scale using several block sizes and $L=1200$. The data for $b=100$, 60, 30, and 15 were averaged over 200, 230, 150, and 100 runs, respectively, and the error bars are about the size of the symbols. $t_0=2000$ is used for these calculations. The figure shows that the temporal correlations decay with the displaced time τ, and the decay gets slower as larger block sizes are used. The curvature in the data points suggests that the decay does not obey a power law. Plotting the data in a log-linear scale does not produce a linear decay either, implying $C(b,\tau)$ does not decay exponentially. Note that beyond $t=2000$, $U(b,t)$ decays very slowly [cf. Fig. 5(c)]. It is this region of U, which has been used to calculate the temporal correlations. A slow decay in U suggests that long-wavelength surface fluctuations are being generated, and therefore the temporal behavior of $C(b,\tau)$ in this region should be important to the growth dynamics.

For this dynamical information to be useful, $C(b,\tau)$ must be independent of L, the lateral extent of the system, while the extensive properties of $C(b,\tau)$ should depend only on the blocksize b. It is important to determine whether $U(b,t)$ contains information that is intrinsic to the dynamics of the system. In Fig. 6(b) we have shown $C(b,\tau)$ vs τ for the EW model using $L=1200$ and $L=600$ for several block sizes.

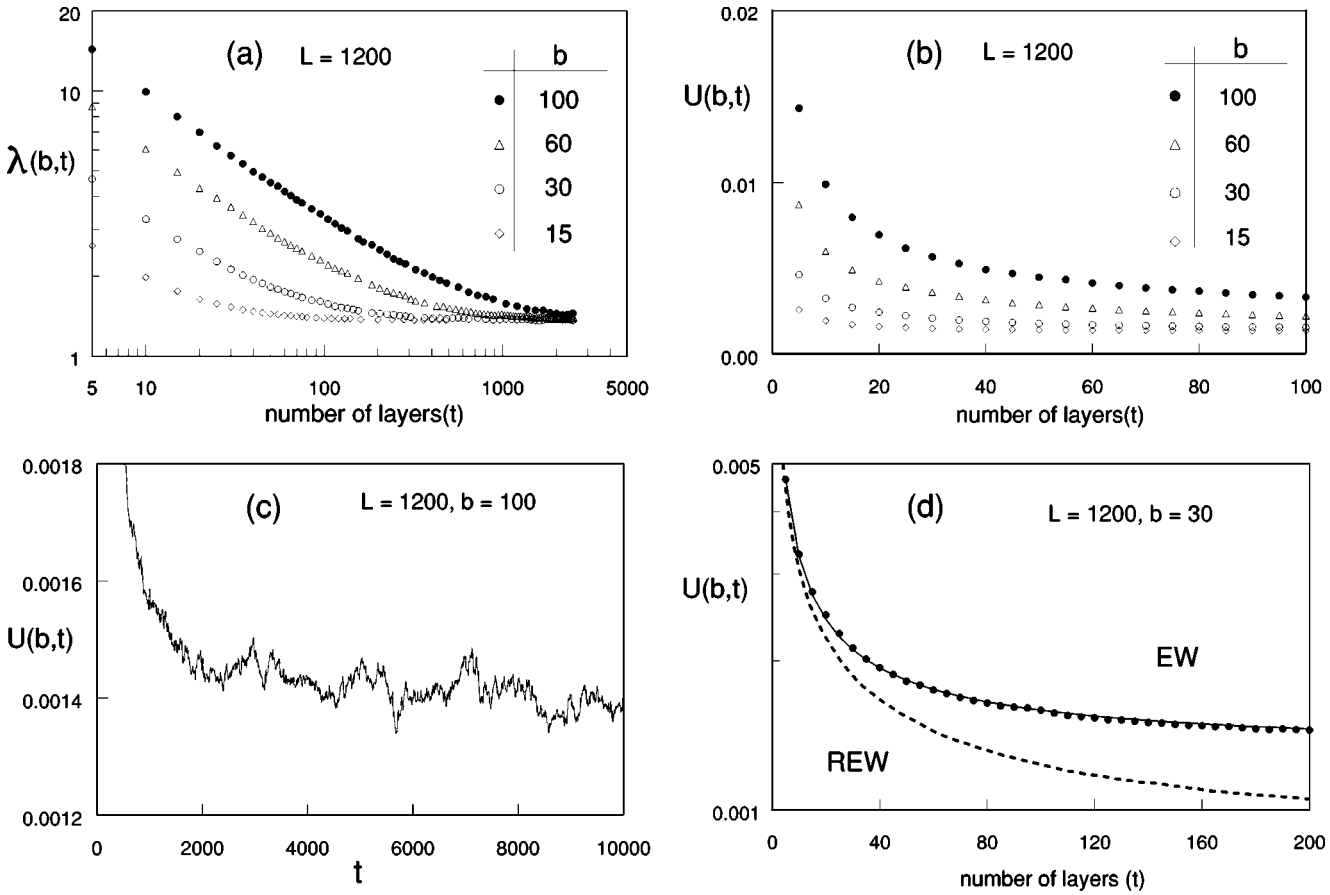

FIG. 5. (a) The surface stiffness $\lambda(b,t)$ for the EW model vs the number of deposited layers. (b) The nonequilibrium dynamical contribution to the interface velocity $U(b,t)$ vs the number of layers deposited using $L=1200$. (c) $U(b,t)$ vs t for the EW model. (d) $U(b,t)$ vs t for the EW and REW models.

The data points for $L=600$ and $b=60$, 30, and 15 were averaged over 120, 80, and 50 runs, respectively. The figure shows that the data for different L, but same block size, fall on the same curve. This implies that $C(b,\tau)$ is independent of L and only depends on b. Additional measurements using $L=1800$ and $b=100$ are in agreement with the above observations.

An important point to note is that $C(b,\tau)$ has to be independent of t_0 [cf. Eq. (16)] for the measurements and dynamical scaling of the temporal correlations to be robust. If the time-dependent correlation $C(b,\tau)$ depends upon two times, it means that the system is still in a transient state. Figure 6(c) shows $C(b,\tau)$ with τ for the EW model in a log-linear scale for different values of t_0. For $t_0=3000$, 2000, 500, and 200, the data points were averaged over 165, 230, 90, and 60 runs, respectively. The figure shows that for small values of t_0 the temporal correlations decay quickly. When larger values of t_0 are used, $C(b,\tau)$ decays slowly and finally approaches a behavior where it is independent of t_0. This is seen in Fig. 6(c) for the two largest values of t_0, where the data points are seen to collapse on the same curve. Another interesting point to note here is that $C(b,\tau)$ decays nonexponentially with τ. A Levenberg-Marquardt fit [30] for the two largest values of t_0 using Eq. (17) yielded excellent fits with high statistical confidence, suggesting that Eq. (17) may be used to study the dynamical scaling properties of $C(b,\tau)$ in the EW model.

In Fig. 6(d) we have plotted $C(b,\tau)$ with τ in a log-linear scale for the REW model using $t_0=4000$. The data points for both $b=100$ and 30 were averaged over 72 runs. After an initial transient, the decay in the data becomes linear, suggesting an exponential decay of temporal correlations at long times. This behavior is better observed for $b=30$ where $C(b,\tau)$ is seen to decay exponentially for $\tau>200$. An exponential decay of the temporal correlations is consistent with the solutions of the linear Langevin equation, which has the dynamic exponent of $z=2.0$.

The calculation of spatial correlations is important in determining whether the dynamical scaling theory we presented in Sec. II is robust. Using $t_0=2000$, we have calculated the space-displaced correlation function $\langle U_q U_{q'}\rangle$, where U_q is the Fourier transform of $U(\mathbf{r},t)$. The spatial correlation function is plotted in Fig. 7(a) for different q values where the data points represent averages over 100 independent runs. For $L=300$ and $b=1$, spatial correlations can be seen in the data for small q, which decay as larger values of q are used. The solid line through the data points is a Gaussian fit using the Levenberg-Marquardt method [30]. When the spatial correlation function is calculated over a coarse-grained lattice using $L=600$ and $b=2$ (i.e., keeping

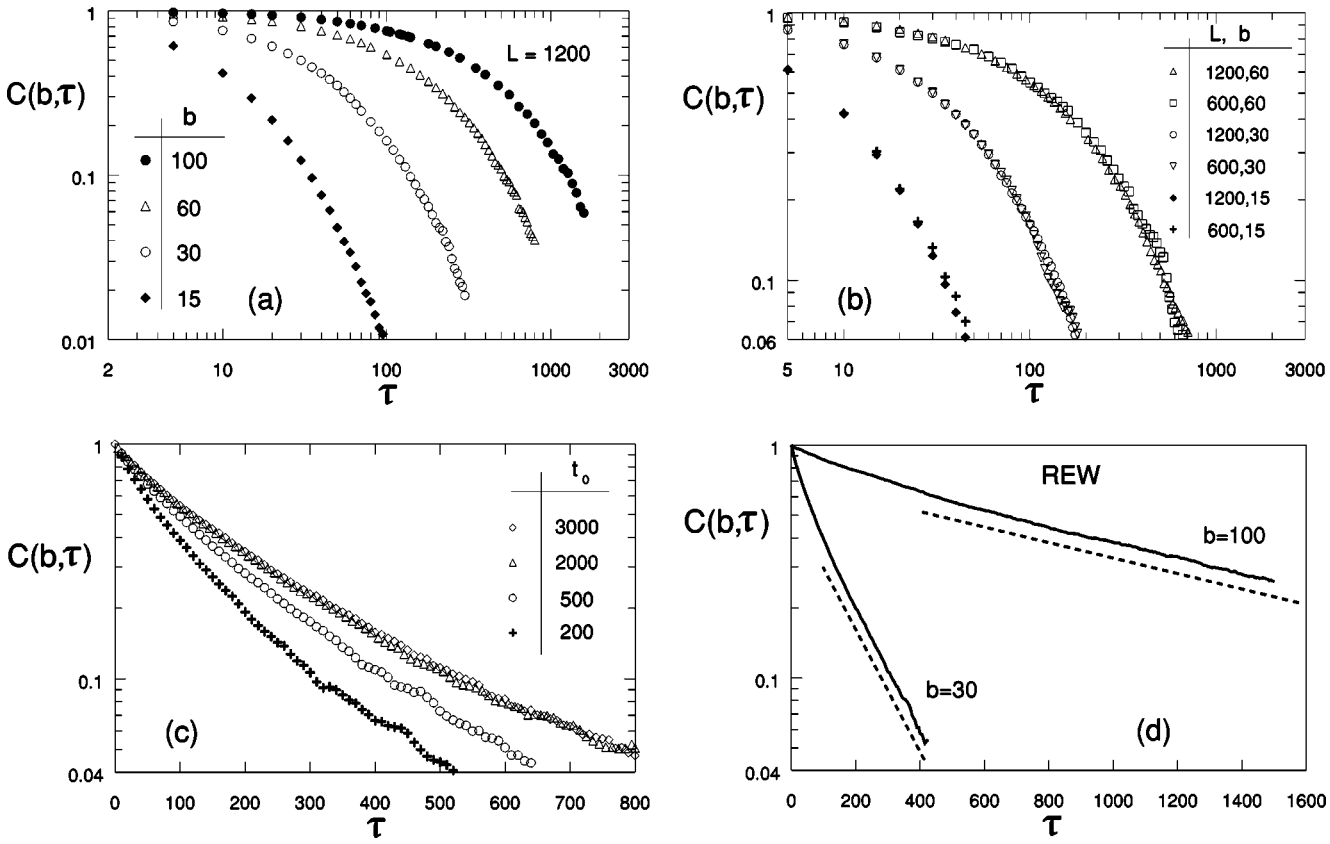

FIG. 6. (a) The time-displaced correlation function $C(b,\tau)$ vs τ for the EW model. (b) $C(b,\tau)$ vs τ for the EW model using several lattice sizes L and block sizes b. (c) $C(b,\tau)$ vs τ for the EW model using $L=1200$, $b=60$, and different values of t_0. (d) $C(b,\tau)$ vs τ for the REW model using $L=1200$. The dotted lines are a guide to the eye.

the overall length same), the correlations do not show any systematic behavior over a wide range of length scales, suggesting that the spatial correlations are random. This demonstrates that nontrivial spatial correlations are not being generated by the model, while also assuring that the random number generator is producing good quality numbers.

We have used larger values of Δt in Eq. (13) to investigate their effects on the time-displaced correlations $C(b,\tau)$. In Fig. 7(b), $C(b,\tau)$ with τ for $\Delta t=1$, 2, and 4 has been plotted using $b=60$. For these runs $L=1200$ is used. Also, $t_0=2000$ and $t_0=4000$ were used for $\Delta t=1$ and $\Delta t=2$, respectively. For $\Delta t=4$ we have used $L=1800$ and $t_0=8000$. The data points for $\Delta t=2$, and $\Delta t=4$ were averaged over 18 and 10 runs, respectively. The figure shows that the behavior of $C(b,\tau)$ with τ is independent of the values of Δt and t_0. We have also performed some additional calculations where deposition of eight monolayers evolved time by one unit. In these studies $L=1800$, $b=300$, and $t_0=500$ are chosen. Due to a higher rate of deposition per unit time, $C(b,\tau)$ for a single run is much noisier as expected. Also, the data deviate from an exponential decay in agreement with the behavior observed in Fig. 6(c).

D. Dynamical scaling of $C(b,\tau)$

For a finite system with lateral length L, the properties of U can be studied by coarse graining the two-dimensional surface into $l\times l$ blocks of blocksize $b=L/l$ and measuring U over the blocksize b. If U is an extensive quantity, then meaningful dynamical information through the measurement of $C(b,\tau)$ can be obtained by studying it over different blocksizes. Note that an analogous process has been used to determine the noise properties of magnetic flux in superconducting Josephson junction arrays (JJA) [31].

The blocked, time-displaced correlation function (neglecting higher-order corrections) can be written generally as

$$C(b,\tau)\sim\tau^{\mu(b)-1}\exp[-\Omega(b)\tau], \tag{18}$$

where $\Omega(b)$ is the blocksize dependent frequency that determines the decay in $C(b,\tau)$ at long times. In Eq. (18) we have assumed a functional form similar to that in Eq. (17), allowing for a dependence of the exponent $\mu(b)$ on the block size b as well. Empirically, we find that a variation linear in the inverse blocksize b^{-1} accounts for the data,

$$\mu(b)=\mu-s/b, \tag{19}$$

where s is a constant. The blocksize b establishes a cutoff for low-frequency fluctuations, and this, in turn, controls the amount of information in $C(b,\tau)$ relevant to the growth behavior at long times. Hence the decay of temporal correlations is determined by the blocksize b.

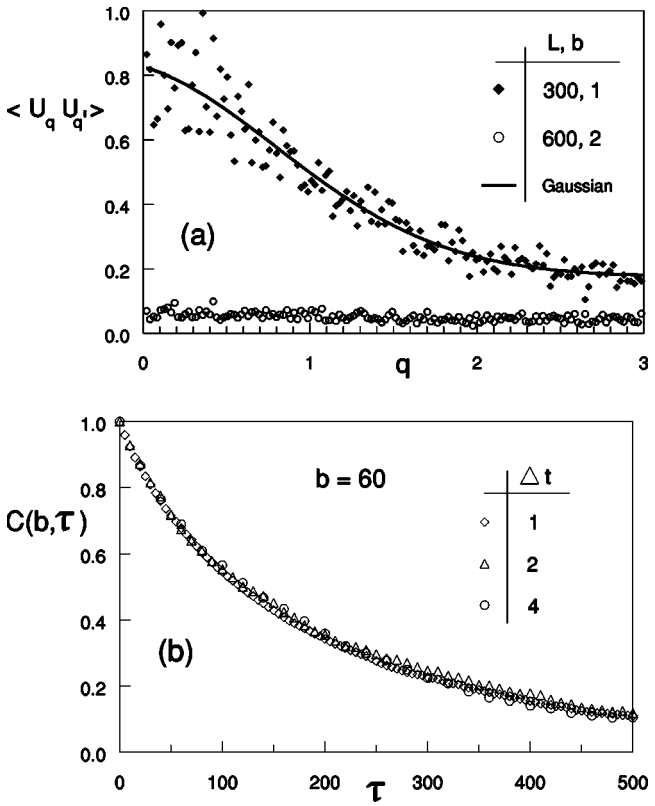

FIG. 7. (a) The space-displaced correlation function of U vs q for the EW model. The solid curve is a Gaussian fit through the data points. (b) $C(b,\tau)$ vs τ for the EW model using different values of Δt.

A general form for a dynamic scaling relation for the function of the time-displaced correlation function is

$$C(b,\tau) \sim b^{z[\mu(b)-1]} F\left(b, \frac{\tau}{b^z}\right), \tag{20}$$

where z is the dynamic exponent. The function

$$F(b,x) = x^{\mu(b)-1} \exp[-\Omega_c x], \tag{21}$$

for $x>0$, and the frequency Ω_c is a constant that characterizes the nonequilibrium fluctuations in a given growth model. The ratio $P(b,\tau)=C(b,\tau)/\tau^{\mu(b)-1}$ simplifies the dependency on τ and b in a manner such that at long times $P(b,\tau)$ decays exponentially and depends *only* on $x=\tau/b^z$. Note that for dynamical scaling to hold, the finite-size dependent frequency $\Omega(b)$ should satisfy a constraint such that

$$\Omega(b) \sim b^{-z} \Omega_c . \tag{22}$$

In order to test for scaling of the temporal correlations in the EW model [Fig. 6(a)], we have to determine the asymptotic value of $\mu(b)$ and the value of the constant s [cf. Eq. (19)]. The data in Fig. 6(a) are therefore fitted (excluding the values for $\tau=0$) to Eq. (17) using the Levenberg-Marquardt method [30]. Comparing Eqs. (17) and (18), we find that $\mu(b)$ and $\Omega(b)$ are given by $a_2=\mu(b)$ and $a_3=\Omega(b)$, respectively. Excellent fits are obtained for different block sizes with high statistical confidence. The values of each of the coefficients a_0 for different block sizes obtained from the fits are less than 0.037 and show no systematic dependence on b. Also, the coefficients $a_1(b)$ are roughly 1 and exhibit no systematic dependency with b. Figures 8(a) and 8(b) show the plots of $a_2=\mu(b)$ and $a_3=\Omega(b)$ vs $1/b$. The straight-line fit through the data points in Fig. 8(a) gives $\mu=0.998\pm0.001$ and $s=2.97\pm0.02$ [cf. Eq. (19)]. In Fig. 8(b), the power-law fit through the data points for $b=100$, 60, and 30 yielded $z=1.65\pm0.04$, and $\Omega_c=4.0\pm1.0$, respectively. Note that Ω_c can be estimated from this figure if the equality $\Omega(b)=b^{-z}\Omega_c$ is assumed to be valid.

Using $z=1.65$ we tested dynamical scaling of the temporal correlations in the EW model, with the results shown in Fig. 8(c). Excellent collapse of the data is obtained for the three largest block sizes over a wide range of τ values. After an initial transient, the data appear to decay exponentially with a slope of ~ 3.0. When $z=2.0$ is used, the data for different block sizes show systematic deviations and fail to collapse onto a single curve [Fig. 8(d)]. The failure of scaling in the EW model with $z=2.0$ agrees with our earlier observations on the scaling of the interfacial width and the structure factor.

V. DISCUSSION

The extensive simulations described above produced precise data for the interfacial width $W(L,t)$ and the structure factor $S(qL,L,t)$ as a function of substrate size L so that a careful finite-size scaling analysis could be carried out. One very important component of this study was the additional determination of the stochastic contribution to the interface velocity $U(b,t)$, a quantity whose temporal correlations can offer insights about the dynamical evolution that are not clarified by the interfacial width or the structure factor.

For the linear Langevin equation [Eq. (1)], $U(b,t)$ is δ correlated in both space and time, implying a random contribution to the growth velocity due to deposition. In the original formulation of Edwards and Wilkinson [15], the growth velocity was written as

$$\frac{\partial h(\mathbf{r},t)}{\partial t} = Fv + Fa^4 \nabla^2 h + \zeta, \tag{23}$$

where F is the deposition rate per unit area, v is the volume increase of the system in unit time, a is the lattice constant, and ζ is the random noise. The effect of deposition is given by $Fv+\zeta$, where the term Fv causes a steady increase in the interface height due to deposition of a certain volume of material. Note that this equation can be transformed into Eq. (1) by using the transformation $h+Fvt \rightarrow h$. In contrast, for the KPZ equation $(\lambda_f/2)(\nabla h)^2+\zeta$ accounts for the effect of deposition, where λ_f is proportional to the deposition rate. The important distinction between these two equations is that in the EW equation the interfacial growth velocity due to deposition does not accurately couple to the internal degrees of freedom of the interface. It is, therefore, questionable whether the EW equation can be used to study far-from-equilibrium growth processes. Measurement of $U(b,t)$ for

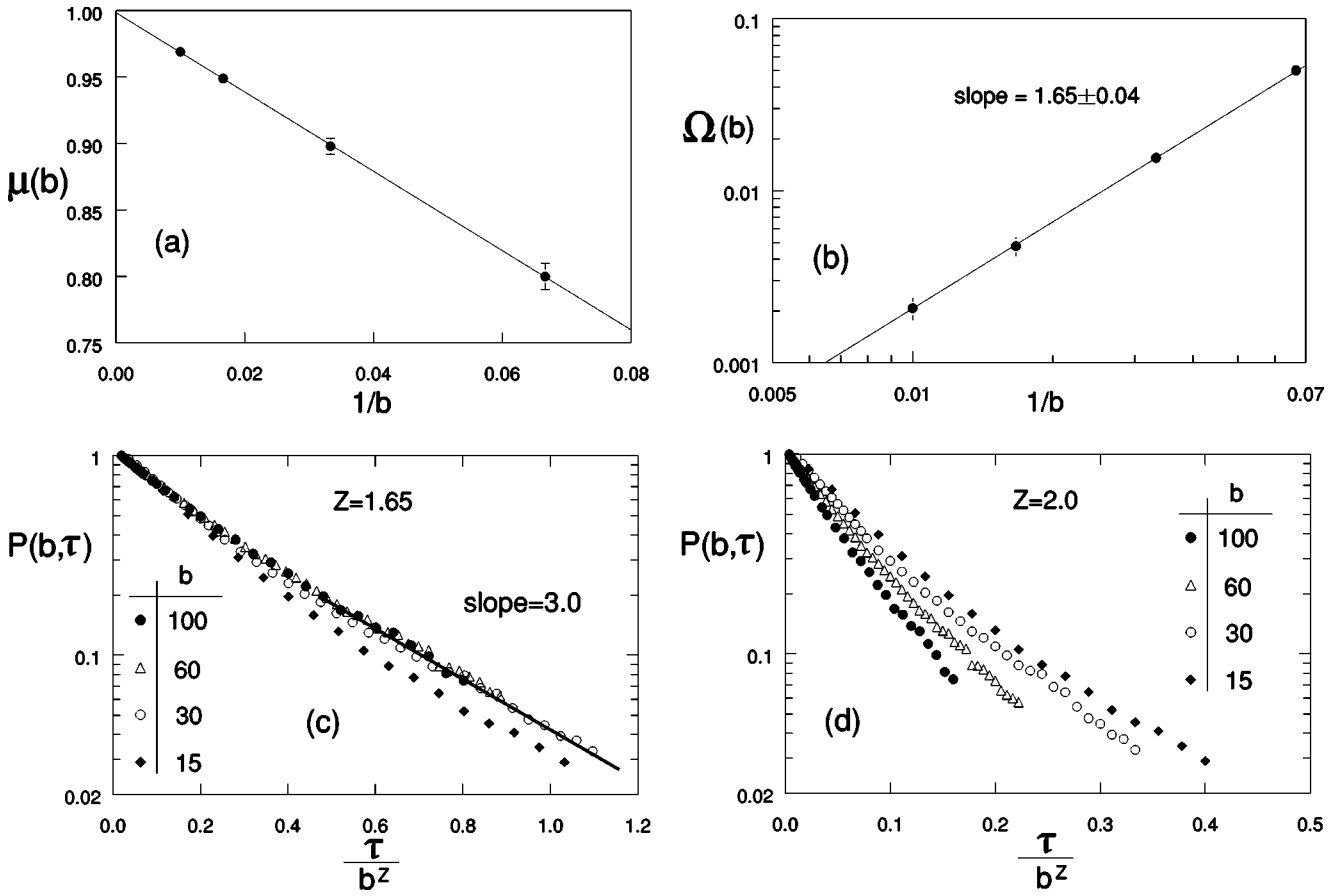

FIG. 8. (a) $\mu(b)$ vs $1/b$ for the EW model in a linear scale. (b) $\Omega(b)$ vs $1/b$ in a log-log scale. (c) Dynamic scaling of the time-displaced temporal correlation function for the EW model using $z=1.65$, $\mu=0.998$, and $s=2.97$. (d) Dynamic scaling of the time-displaced temporal correlation function for the EW model using $z=2.0$, $\mu=0.998$, and $s=2.97$.

the atomistic EW model demonstrates the shortcomings of the EW equation. Also, it should generally provide a better estimate of the stochastic contribution to growth than the phenomenological term used in the KPZ equation.

The extensive computer simulations described above revealed nonequivalent dynamical behaviors for the EW and REW models, and this difference has two important implications. First, it suggests that minor but ''essential'' differences in the local dynamics can influence time-dependent behavior in nonequilibrium systems. This is contrary to the behavior one normally expects in systems under equilibrium conditions and near the critical point, i.e., $\xi_{\parallel}\sim L$. Second, by observing the differences in the local dynamics in these two models, we may be able to define a mechanism by which surface shape fluctuations become correlated as the surface grows. This, in turn, may explain why z for the atomistic EW model is different from 2.0.

A possible explanation for the uncorrelated evolution of surface fluctuations in the REW model is that the growth dynamics in the REW model may be viewed as a two-step process: (1) a particle is deposited randomly on the surface; (2) the particle is then moved *only if* a suitable site is found, which is at the lowest depth and not in competition with any neighboring sites. The net effect of step (1) is to produce uncorrelated surface fluctuations. If step (2) is possible, the particle move then contributes only deterministically to the surface shape. The state of the surface shape at time t may be characterized by a functional $S(h_1,h_2,\ldots h_i,t)$, where h_i's are the heights at different sites. For the REW model, h_i is nondegenerate, implying that there is only one way the surface can evolve from state to state so that the surface shape evolves deterministically from one discrete time to another. Thus, if information on the sites where particles are randomly deposited are available (sequentially within a time interval Δt), it will enable to reverse the surface shape by reversing time. Since deposition causes random fluctuations in the surface shape, the net effect of deposition and surface diffusion in the REW model results in surface shapes that correlate in a simple manner during growth.

In contrast, for the EW model h_i is degenerate, allowing for many possibilities from which the surface shapes can evolve from state to state. This property of the local diffusion dynamics in the EW model makes it impossible to reverse the surface shape by simply reversing time, even if information is kept on the sites where particles are randomly deposited (sequentially within a time interval Δt.) The overall effect is to generate nontrivial correlations with surface shapes at previous times. Although ''layer-by-layer''-like oscillations were seen in the early time simulation data for the interfacial width for the EW model, these die away rather

quickly. This behavior suggests that lattice effects [32] could differentiate the EW model from a continuum model. However, the rms interfacial width is of order unity for both the EW and REW models, and we believe that the relatively small difference is unlikely to account for the difference in measured values of z. From the existing data for the EW we estimate that approximately 10^{12} layers would have to be grown for the interfacial width to reach the values we found for the REW model. This is clearly beyond our ability to simulate with current resources. Although we could simply remove the lattice restriction to test for lattice effects, such a modification would also eliminate the degeneracy in energy amongst nearest-neighbor sites and change the diffusion in a fundamental way. We also note that similar behavior to what we found for the EW model has been seen in molecular beam epitaxy (MBE) growth simulations using lattice models for which the interfacial width becomes large compared to the lattice constant, yet dynamic scaling is still found with $z=1.65$. We thus conclude that it is unlikely that lattice effects are responsible for the difference in dynamic exponent between the EW and REW models. Of course, we cannot exclude the possibility that our data are not yet in the asymptotic regions of size and time; however, our rather massive simulation gave no hint of any crossover to another regime. This suggests that if crossover does occur, several orders of magnitude more effort will be needed to detect it and there is little hope of doing so in the near future. Thus, we believe that the most likely explanation for the differences between the EW and REW models results from the nontrivial correlations that we have found in the coarse-graining analysis.

VI. CONCLUSIONS

We have presented extensive simulations of the $2+1$ dimensional atomistic EW and REW models using lattice sizes as large as $L=1800$, although only data for sizes as large as $L=1280$ were presented in the manuscript. For each model self-consistent dynamic finite size scaling was obtained for both the structure factor and interfacial width with a dynamic exponent of $z=1.65\pm0.05$ for the EW model but $z=2.0\pm0.1$ for the REW model. No hint of crossover to different behavior was seen for the largest lattices, even after 10^3–10^4 layers were deposited. The local diffusion dynamics in the EW model show nontrivial temporal correlations, and this is likely to explain why the atomistic EW model dynamic exponent differs from that for the continuum EW equation or the REW model. This also implies that the kinetic Monte Carlo studies of MBE models should be expected to find that z differs from that for the continuum EW equation, since randomness in the diffusion is an essential feature of the models.

ACKNOWLEDGMENTS

This research was supported in part by NSF Grant Nos. DMR-9727714 and DMR-0094422. S.P. gratefully acknowledges funding at Pennsylvania State University from NASA and the Petroleum Fund administered by the American Chemical Society.

[1] See, e.g., X.M. Yang, K. Tonami, L.A. Nagahara, K. Hashimoto, Y. Wei, and A. Fujishima, Surf. Sci. **319**, L17 (1994); O. Vatel, E. Andre, F. Chollet, P. Dumas, and F. Salvan, J. Vac. Sci. Technol. B **12**, 2037 (1994).
[2] *Solids Far From Equilibrium*, edited by C. Godréche (Cambridge University Press, New York, 1992).
[3] S. Pal and D.P. Landau, Physica A **267**, 406 (1999).
[4] D. Liu and M. Plischke, Phys. Rev. B **38**, 4781 (1988).
[5] P. Dutta and P.M. Horn, Rev. Mod. Phys. **53**, 497 (1981).
[6] M.J. Johnson and D.M. Fleetwood, Appl. Phys. Lett. **70**, 1158 (1997).
[7] T.J. Shaw, M.J. Ferrari, L.L. Sohn, D.-H. Lee, M. Tinkham, and J. Clarke, Phys. Rev. Lett. **76**, 2551 (1996).
[8] M. Takayasu, H. Takayasu, and T. Sato, Physica A **233**, 824 (1996).
[9] M. Kardar, G. Parisi, and Y.-C. Zhang, Phys. Rev. Lett. **56**, 889 (1986).
[10] J. Krug, Phys. Rev. A **44**, R801 (1991).
[11] E. Medina, T. Hwa, M. Kardar, and Y.-C. Zhang, Phys. Rev. A **39**, 3053 (1989).
[12] J. Krug, J. Phys. A **22**, L769 (1989); J. Krug and H. Spohn, Phys. Rev. Lett. **64**, 2332 (1990); Europhys. Lett. **8**, 219 (1989).
[13] F. Family, J. Phys. A **19**, L441 (1986).
[14] L. Sander, in *Solids Far From Equilibrium*, edited by C. Godréche (Cambridge University Press, New York, 1992), p. 434.
[15] S.F. Edwards and D.R. Wilkinson, Proc. R. Soc. London, Ser. A **381**, 17 (1982).
[16] F. Family and T. Vicsek, J. Phys. A **18**, L75 (1985).
[17] M. Plischke and Z. Racz, Phys. Rev. A **32**, 3825 (1985).
[18] H. Guo, B. Grossman, and M. Grant, Phys. Rev. Lett. **64**, 1262 (1990).
[19] P. Meakin, P. Ramanlal, L.M. Sander, and R.C. Ball, Phys. Rev. A **34**, 5091 (1986).
[20] J.M. Kim and J.M. Kosterlitz, Phys. Rev. Lett. **62**, 2289 (1989).
[21] L.-H. Tang, B.M. Forrest, and D.E. Wolf, Phys. Rev. A **45**, 7162 (1992).
[22] M. Plischke, Z. Racz, and D. Liu, Phys. Rev. B **35**, 3485 (1987).
[23] S. Pal and D.P. Landau, Phys. Rev. B **49**, 10 597 (1994).
[24] D.E. Wolf and J. Villain, Europhys. Lett. **13**, 389 (1990).
[25] L. Brendel, H. Kallabis, and D.E. Wolf, Phys. Rev. E **58**, 664 (1998).
[26] R.S. Ross and M.F. Gyure, Phys. Rev. B **61**, 8602 (2000).
[27] T. Nattermann and L.-H. Tang, Phys. Rev. A **45**, 7156 (1992).
[28] B.M. Forrest and L.-H. Tang, J. Stat. Phys. **60**, 181 (1990).
[29] B.I. Halperin and P.C. Hohenberg, Rev. Mod. Phys. **49**, 435 (1977).

[30] *Numerical Recipes: The Art of Scientific Computing*, edited by W.H. Press, B.P. Flannery, S.A. Teukolsky, and W.H. Vetterling (Cambridge University Press, New York, 1989).
[31] P.H.E. Tiesinga, T.J. Hagenaars, J.E. van Himbergen, and Jorge V. Jose, Phys. Rev. Lett. **78**, 519 (1997).
[32] See e.g., H. Kallabis, Int. J. Mod. Phys. B **11**, 3621 (1997); M. Rost and J. Krug, J. Phys. I **7**, 1627 (1997); L. Brendel, H. Kallabis, and D.E. Wolf, Phys. Rev. E **58**, 664 (1998).